

Novel Direct Alpha Spectroscopy Technique for ^{225}Ac Radiopharmaceutical detection in Cancer Cells

Mahsa Farasat^a, Behrad Saeedi^b, Luke Wharton^b, Sidney Shapiro^d,
Chris Vinnick^c, Madison Daignault^c, Meghan Kostashuk^{g,b},
Nicholas Pranjatno^e, Myla Weiman^a, Corina Andreoiu^c, Hua
Yang^{b,c,f}, Peter Kunz^{a,c}

^a Accelerator Division, TRIUMF, 4004 Wesbrook Mall, Vancouver, BC V6T 2A3, Canada

^b Life Sciences Division, TRIUMF, 4004 Wesbrook Mall, Vancouver, BC V6T 2A3, Canada

^c Department of Chemistry, Simon Fraser University, Burnaby, BC V5A 1S6, Canada

^d Physics and Astronomy, University of British Columbia, Vancouver, BC V6T 1Z4, Canada

^e Department of Physics, Simon Fraser University, Burnaby, BC V5A 1S6, Canada

^f Department of Chemistry, University of British Columbia, Vancouver, BC V6T 1Z1, Canada

^g McMaster School of Biomedical Engineering, McMaster University, Hamilton, Ontario L8S 4L7, Canada

E-mail: mfarasat@triumf.ca

Abstract. Targeted alpha-particle therapy (TAT) employs alpha-emitting radionuclides conjugated to tumor-targeting molecules to deliver localized radiation to cancer cells, showing great promise in treating metastatic cancers. Among these radionuclides, Actinium-225 (^{225}Ac , $t_{1/2} = 9.9$ days) has emerged as a clinically promising candidate. Its decay chain generates four successive alpha emissions, resulting in highly localized and effective cytotoxic damage to cancer cells when delivered to tumor sites. However, the assumption of complete retention of ^{225}Ac and its radioactive daughters at these target sites is often inaccurate. The nuclear recoil effect can lead to off-target distribution and unintended toxicity.

To address this challenge, we developed a novel direct alpha spectroscopy method utilizing the Bio-Sample Alpha Detector (BAD). Alpha emission spectra were acquired under atmospheric pressure at room temperature, enabling direct observation of ^{225}Ac and its daughters' behavior in radiopharmaceutical applications. AR42J rat pancreatic tumor cells, expressing somatostatin receptor 2 (SSTR2), were incubated with [^{225}Ac]Ac-crown-TATE, [^{225}Ac]Ac-PSMA-617, and [^{225}Ac]Ac³⁺. The BAD setup allowed placement of radiolabeled cell samples within 100 μm of the detector, facilitating alpha spectra acquisition with statistical uncertainties <1%.

Our results revealed distinct spectral differences between radiolabeled cells and reference samples, demonstrating [^{225}Ac]Ac-crown-TATE uptake by AR42J cells. Detection of ^{213}Po , one of the ^{225}Ac decay daughters, highlighted partial retention and release of decay products from cells, providing information on intracellular retention and daughter redistribution. Geant4 simulations confirmed the alignment of experimental data with theoretical models,

validating the method's accuracy. This study establishes a direct alpha spectroscopy approach for investigating ^{225}Ac and its daughters' behavior in cells and offers a powerful tool for microdosimetry estimation.

Keywords: Ac-225, cancer cells, Targeted alpha therapy, Alpha detector

1. Introduction

The field of radiopharmaceuticals has witnessed significant advancements in recent years, particularly in the development of alpha-emitting isotopes for Targeted Alpha Therapy (TAT). TAT leverages the high linear energy transfer (LET) and short range of alpha particles to selectively destroy cancer cells while minimizing damage to surrounding healthy tissue [1, 2, 3]. This approach shows particular promise for treating metastatic and micro-metastatic cancers, which often prove resistant to conventional therapies [4]. Alpha particles, characterized by energies typically ranging from 3 to 10 MeV, exhibit a high LET and a short range in biological tissues ($<100\ \mu\text{m}$). These properties enable the delivery of highly localized and lethal radiation doses, inducing severe DNA damage in targeted cells. However, these same properties pose challenges in research, as their short range complicates direct detection, particularly in biological environments where attenuation and scattering can hinder accurate measurements [5]. One alpha-emitting isotope that has gained considerable attention for its therapeutic properties is Actinium-225 (^{225}Ac). ^{225}Ac has shown significant promise for clinical applications due to its relatively long half-life of approximately 10 days. This provides a potentially suitable balance between allowing sufficient time for targeted delivery and sustaining therapeutic activity. The decay chain of ^{225}Ac includes the emission of four alpha particles with energies ranging from 5.8 MeV to 8.4 MeV, each of which is highly effective in inducing double-strand breaks in the DNA of cancer cells, ultimately leading to cell death. This makes ^{225}Ac -labeled radiopharmaceuticals particularly effective in treating cancers such as prostate cancer and neuroendocrine tumors [2, 6]. Despite its advantages, the application of ^{225}Ac -based therapies faces key challenges, particularly in the detection and measurement of alpha emissions in biological systems [6]. One significant challenge is that ^{225}Ac -labeled complexes contain up to seven radioisotopes in their decay chain. The high recoil energy of alpha decay can break coordination bonds, leading to the release of uncomplexed daughter radionuclides. These progenies may redistribute in vivo, making accurate microdosimetry estimation challenging. The redistribution of these daughter radionuclides is still not well understood, adding complexity to dosimetry and potential toxicity assessments [7].

Conventional measurement techniques often rely on indirect gamma detection [8], which is problematic for isotopes like ^{225}Ac that emit alpha particles without easily detectable gamma rays. This limitation prevents real-time monitoring of the behavior and function of alpha emitters in biological systems. Furthermore, conventional alpha detectors, while

effective in industrial and scientific settings, are not well-suited for use in biological studies. These detectors typically operate under a vacuum to minimize attenuation, making them incompatible with measurements in living cell cultures. Addressing these challenges requires innovative detection methods that can provide direct and real-time insights into alpha-emitting isotopes under biologically relevant conditions.

This study aims to develop a Bio-Sample Alpha Detector (BAD) and novel measurement protocols that enable *in vitro* investigation of ^{225}Ac -labeled pharmaceuticals. As a spin-off of a research project related to medical isotopes, we leveraged expertise and technology from the characterization of radioactive ion beams to develop the BAD for direct alpha spectroscopy on cell cultures. By focusing on the development of a silicon PIN (SiPIN) sensor-based alpha detector capable of operating at ambient temperature and normal atmospheric conditions, we investigated the alpha spectra of pancreatic cancerous cells incubated with labeled ^{225}Ac . This approach represents a significant step forward in the field, as it not only enhances our understanding of the behavior of alpha-emitting radiopharmaceuticals in a biological context but also reduces the reliance on animal models. Such advancements contribute to a more ethical and potentially more accurate assessment of therapeutic efficacy.

Section 2 outlines experimental configurations and procedures, including a Geant4 simulation of the detector response. Geant4, short for Geometry and Tracking, is a Monte Carlo-based toolkit developed by CERN for simulating the passage of particles through matter, widely used in high-energy physics, medical physics, and space science. In Section 3, experimental data is analyzed, and results are discussed. Section 4 includes a summary and an outlook towards further developments and applications.

2. Experimental

2.1. Material and instruments

Unless otherwise specified, all solvents and reagents were obtained from commercial suppliers. The F12K Nutrient Mixture (1X), Dulbecco's Modified Eagle Medium (DMEM (1X)), Dulbecco's Phosphate Buffered Saline (DPBS (1X)), Fetal Bovine Serum (FBS), Penicillin-Streptomycin (PS), and Trypsin-EDTA (0.25%) were purchased from Gibco (USA). The AR42J pancreatic tumor cell line was obtained from Cedarlane Corporation (Canada). The crown-TATE targeting agent was synthesized in-house at TRIUMF by Wharton et al [9]. The PSMA targeting agent was purchased from MedChemExpress. Ammonium acetate (NH_4OAc , trace metal grade), poly-D-lysine, and EDTA were supplied by Sigma-Aldrich. Standard 24-well plates and 150 mm plates, used for routine cell cultures, were purchased from Thermo Fisher Scientific. Radiolabeling studies were analyzed using instant thin-layer chromatography (iTLC) with salicylic acid (SA) impregnated TLC plates (Agilent Technologies). The plates were imaged with an AR2000 TLC scanner (Eckert & Ziegler) equipped with P10 gas and WinScan V3.14 software. Activities of ^{225}Ac were quantified using a high-purity germanium (HPGe) detector (Mirion Technologies, Canberra Inc.),

which was calibrated with standardized ^{152}Eu and ^{133}Ba sources in a fixed geometry (20 mL scintillation vials) at specified sample heights [10, 11]. Samples containing ^{225}Ac were diluted into 20 mL scintillation vials (in H_2O), and gamma emission spectra were recorded after secular equilibrium with daughter radionuclides had been reached. All spectra were acquired with a dead time of less than 1.5%. Radionuclide activities were calculated using Genie 2000 software, which utilized a radioisotope library containing key gamma emission lines of ^{221}Fr (218 keV) and ^{213}Bi (440 keV). A Countess 3 automated cell counter, along with Countess cell counting chamber slides (Thermo Fisher Scientific), was used to count cells throughout the experiment. A standard inverted light microscope equipped with a camera was employed to monitor cell cultures, while centrifuges capable of spinning 15 mL and 50 mL Falcon tubes, as well as Eppendorf tubes, were used to create cell pellets. All cell cultures were conducted within a certified level 2 biological safety cabinet (BSC). An Isotemp CO_2 incubator maintained at 37 °C with 5% CO_2 was used for incubating all cell cultures.

All experimental work was performed in the radiochemistry and cell biology laboratories of TRIUMF's Life Sciences Division.

2.2. Bio-sample Alpha Detector

The BAD utilizes a HAMAMATSU S-series Si PIN photodiode with an active area of 18×18 mm [12]. This photodiode was connected to a Mesytec MSI-8 preamp-shaping amplifier module. A stable bias voltage of +70 V was supplied to the detector using a high voltage power supply from Mesytec. The processed signal from the photodiode was then sent to a 12-bit multi-channel analyzer (Toivel ADC/MCA). Data acquisition was managed with a custom software package using CERN's ROOT data analysis framework and MIDAS that was adapted for this specific application [13]. For optimal performance, the design of the sample cups was critical. We used SpectroMicro XRF sample cups with dimensions of 23.9 mm \times 18.4 mm (outer diameter) \times 19.4 mm (height), equipped with a 2.5 μm thick Mylar foil layer (Figure 1a). The choice of Mylar foil was crucial, as its thinness allows alpha particles to pass through with minimal energy loss, ensuring accurate detection. Additionally, the detector setup was specifically designed to minimize the distance between the radioactive source and the detector, achieving a source-to-detector separation of approximately 100 μm . The detection system was then calibrated for energy and efficiency using a ^{225}Ac calibration source prepared by drying a ^{225}Ac solution of known activity in SpectroMicro XRF sample cups. A CAD schematic view of the detector assembly is shown in Figure 1b.

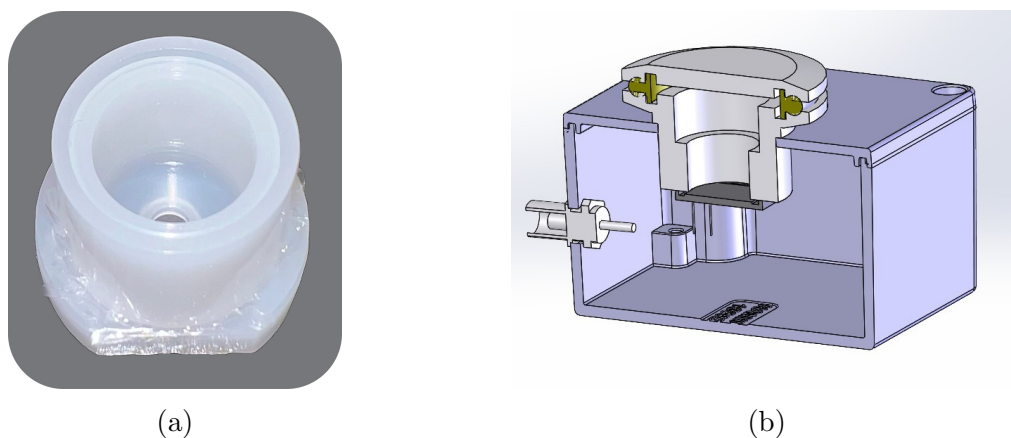


Figure 1: **(a)**: SpectroMicro XRF sample cup with a Mylar foil layer at the bottom, used for cell sample preparation in direct alpha spectroscopy. The cup dimensions are 23.9 mm \times 18.4 mm (outer diameter) \times 19.4 mm (height), with a Mylar foil thickness of 2.5 μm to ensure optimal alpha particle detection. **(b)**: CAD 3D cross section view of the detector assembly.

2.3. ^{225}Ac Production

The ISAC (Isotope Separation and Acceleration) facility at TRIUMF has recently commenced supplying radionuclides for pre-clinical nuclear medicine research. By irradiating ISOL (Isotope Separation OnLine) targets with a 480 MeV proton beam from the TRIUMF H^- cyclotron, the facility is capable of producing a diverse range of radioactive isotope beams (RIBs). For the production of ^{225}Ac , composite ceramic uranium carbide targets are employed. These targets typically have thicknesses ranging from 0.05 to 0.1 mol U/cm^2 and are irradiated with a proton beam at a maximum current of up to 20 μA at an operating temperature of approximately 1950 $^\circ\text{C}$.

A mass-separated RIB of $^{225}\text{Ac}/^{225}\text{Ra}$ isotopes is collected at the ISAC Implantation Station, as detailed in [14]. The ^{225}Ac is then used either directly or extracted from a ^{225}Ra generator for experiments in this study [15]. In addition to ISAC, ^{225}Ac was also sourced from the TRIUMF 520 MeV Isotope Production Facility (IPF). Here, ^{225}Ac was produced by irradiating ^{232}Th foils with a ~ 480 MeV proton beam, with a total irradiation dose of up to 12,500 μAh [16, 10].

2.4. Radiolabeling of ^{225}Ac -Labeled Crown-TATE and PSMA-617

The radiolabeling procedures for both crown-TATE and PSMA-617 with ^{225}Ac followed similar protocols, with the primary difference being the reaction temperatures used for each compound. crown-TATE (10^{-4} M, 2.5 μL) or PSMA-617 (10^{-4} M, 2.5 μL) was combined with ^{225}Ac (18 kBq/ μL , 3.5 μL) in NH_4OAc buffer (pH 7, 5 μL) and distilled water (9 μL) at room temperature. For crown-TATE, the reaction mixture was gently shaken

and incubated at 37 °C for 15 minutes, whereas for PSMA-617, incubation occurred at 90 °C for 15 minutes [17, 18]. To analyze the radiolabeled products, a 2 μ L aliquot of the resulting ^{225}Ac -labeled compound was spotted onto silicic acid-impregnated iTLC plates and developed using EDTA solution (50 mM, pH 5.5). Under these conditions, free ^{225}Ac migrated with the solvent front ($R_f = 1.0$), while both ^{225}Ac -crown-TATE and ^{225}Ac -PSMA-617 remained near the baseline ($R_f = 0.0$ – 0.1). The TLC plates were imaged with an AR2000 TLC scanner (Eckert & Ziegler) using P10 gas and WinScan V3_14 software. To ensure accurate determination of radiochemical yields (RCYs), iTLC imaging of the ^{225}Ac -labeled products was performed after a 4-hour delay, allowing for the decay of free ^{221}Fr ($t_{1/2} = 4.80$ min) and ^{213}Bi ($t_{1/2} = 45.6$ min).

The molar activity of the radiolabeled compounds was determined using the ratio of the activity of ^{225}Ac to the number of moles of targeting agent used for labeling. In this study, a molar activity of 256 kBq/nmol was achieved for both crown-TATE and PSMA-617 and used for subsequent experiments.

^{225}Ac -labeled compounds were diluted in PBS solution to reach the desired volume for the experiment. The diluted activities were further quantified via gamma spectroscopy using a high-purity germanium (HPGe) detector.

2.5. Cell sample preparation

2.5.1. Culturing and Maintenance of AR42J Cells

The AR42J cell line is an epithelial-like cell isolated from a rat's pancreas with a tumor [19]. The cells were cultured in a mixture of 60% (v/v) Ham's F-12K (Kaighn's) Medium and 40% (v/v) Dulbecco's Modified Eagle's Medium (DMEM) on 60 mm plates. The cultures were incubated at 37 °C in a 5% CO_2 environment. Both media were supplemented with 10% (v/v) Fetal Bovine Serum (FBS) and 1% (v/v) Penicillin-Streptomycin (PS) prior to being combined in a 60/40 ratio. AR42J cells are adherent, attaching firmly to the bottom of the culture plates, and exhibit a high density of somatostatin receptor 2 (SSTR2) on their membranes, allowing them to specifically recognize and bind to the crown-TATE peptide. The culture medium was refreshed every two days, and cells were passaged weekly upon reaching approximately 80% confluency. For passaging, the spent medium was first removed, and the cells were washed with 10 mL of PBS to remove residual serum. The cells were then detached by adding 2 mL of trypsin and incubating at 37 °C for 5 minutes. Trypsinization was neutralized by adding 8 mL of media, and the resulting cell suspension was transferred to a Falcon tube. The tube was centrifuged at 1300 RPM for 6 minutes. Following centrifugation, the supernatant containing the media and trypsin was discarded, and the cell pellet was resuspended in 10 mL of fresh media. Finally, the cells were seeded onto 100 mm plates with an appropriate dilution factor, typically a 1:2 ratio if passaged every seven days, depending on the confluency of the original plate.

2.5.2. Preparation of Cell Samples for Direct Alpha Spectroscopy

Figure 2 shows Workflow for the preparation and measurement of AR42J cell samples for alpha spectroscopy. The process began with the removal of the cell culture dish containing the AR42J cell line from the CO₂ incubator. The supernatant media was removed, and the cells were washed with 10 mL of PBS. Then, the cells were detached from the plate by adding 2 mL of trypsin and incubating at 37 °C for 5 minutes. The trypsin was then neutralized using 8 mL of media, the cell suspension was transferred to a Falcon tube, and the Falcon tube was taken to the centrifuge. The cells were centrifuged for 6 minutes at 1300 RPM. After centrifugation, the media/trypsin supernatant solution was removed, and the cells were resuspended in 5 mL of fresh media. An aliquot of the cell suspension was taken, and the cells were counted using the Countess FL 3. Based on the cell concentration obtained, 300,000 cells were seeded in each well of a 24-well plate. The cells were incubated at 37 °C for two days to allow sufficient time for cell adhesion and monolayer formation prior to further experimental procedures.

On the day of the experiment, the media (F12K and DMEM) in each well was carefully removed without disturbing the adherent cell monolayer. 400 μ L of the labeled activity, which was diluted in PBS, was added to each well, and the cells were incubated at 37 °C for an hour. Following incubation, the supernatant containing unbound radiolabel was removed, and 200 μ L of trypsin was added to each well to detach the cells from the surface. The well plate was kept in the incubator for 5 minutes to facilitate cell detachment. To neutralize the trypsin, 800 μ L of fresh media was added to each well, bringing the total volume to 1 mL. The cell suspension was then transferred to an Eppendorf tube and centrifuged at 10 G for 6 minutes. After centrifugation, the supernatant was collected in another Eppendorf tube for further analysis, and 400 μ L of fresh media was added to resuspend the cell pellet. The final cell suspension was thoroughly mixed and transferred to SpectroMicro XRF sample cups, which had been pre-coated with poly-D-lysine to promote cell adhesion. It is worth mentioning Simpler methods such as growing cells on Mylar foil directly, proved inefficient due to ²²⁵Ac's adherence to Mylar, motivating the development of this refined protocol.

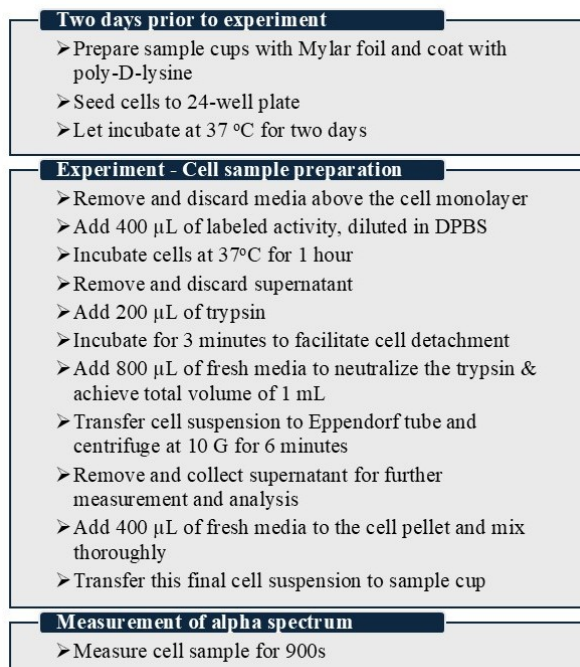


Figure 2: Workflow for the preparation and measurement of AR42J cell samples for alpha spectroscopy.

2.5.3. Direct Alpha Spectroscopy of Cell Cultures Incubated with Labeled Activity

Three sets of sample cups were prepared as described in Section 2.5. The first set contained $[^{225}\text{Ac}]\text{Ac-crown-TATE}$, the second set contained $[^{225}\text{Ac}]\text{Ac-PSMA-617}$ as a negative control (assuming the AR42J cells do not have receptors for PSMA-617), and the third set was incubated with $[^{225}\text{Ac}]\text{Ac}^{3+}$. For each set, a corresponding series of reference sample cups was prepared with the same amount of labeled activity and following the same procedure, but without cells. Each sample cup was placed on the detector, and spectra were acquired for 900 seconds, achieving a statistical uncertainty of less than 1%. The experiment was repeated three times, and the standard deviation was applied to the results. Figure 3 illustrates a schematic view of the experimental setup.

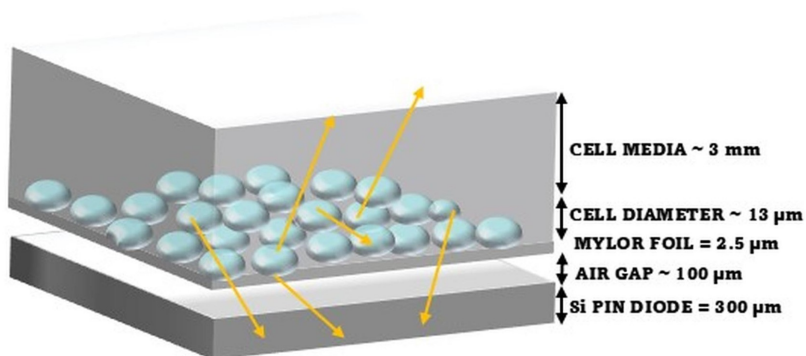


Figure 3: Schematic view of the experimental setup for direct alpha spectroscopy, showing the arrangement of AR42J cells with an approximate diameter of 13 μm . The cells are placed on a 2.5 μm Mylar foil, with a 100 μm air gap separating the cell sample and the Si PIN diode (300 μm thickness). The media layer above the cells is approximately 3 mm thick. The yellow arrows represent the trajectory of emitted alpha particles.

2.5.4. Geant4 simulation

In this study, we employed the Geant4 Monte Carlo simulation toolkit (version 11.2.2) to model the interaction of the radioisotope ^{225}Ac in an aqueous solution with a silicon photodiode detector. Geant4 is a widely used tool for simulating the passage of particles through matter, allowing for detailed predictions of particle interactions within various materials [20]. To simulate the physics of the system, we used a custom physics list that included several physics processes critical to our study: electromagnetic interactions (via the G4EmStandardPhysics class), optical photon interactions (G4OpticalPhysics), radioactive decay processes (G4RadioactiveDecayPhysics), and general particle decay (G4DecayPhysics). Given the complexity of accurately simulating biological cells at the microscale, we used varying thicknesses of water layers, representing different depths from the bottom of the sample cups, as an alternative for cell layers. This approach enabled a more realistic approximation of the experimental conditions and facilitated comparison between the simulated energy spectra and experimental results.

The silicon photodiode detector used in the simulation had dimensions of 18×18 mm and a thickness of 300 μm . A cylindrical sample cup with a diameter of 13 mm and a length of 3 mm was separated by a 100 μm air gap from the detector surface. A Mylar foil with a thickness of 2.5 μm was placed at the bottom of the sample cups. The ^{225}Ac was randomly distributed within the aqueous solution inside the sample cups. By varying the thickness of the water layers, we explored how interaction depth affects the energy spectrum detected by the silicon photodiode, providing valuable insights into the behavior of ^{225}Ac under different conditions. Two sets of simulations were performed: in one, the ^{225}Ac was distributed on the Mylar foil, and in the other, the ^{225}Ac was distributed in a 13 μm water solution depth,

representing the cell diameter. Figure 4 shows the Geant4 simulation geometry. Simulated spectra are included in Figure 11 and Figure 12 in comparison to experimental results.

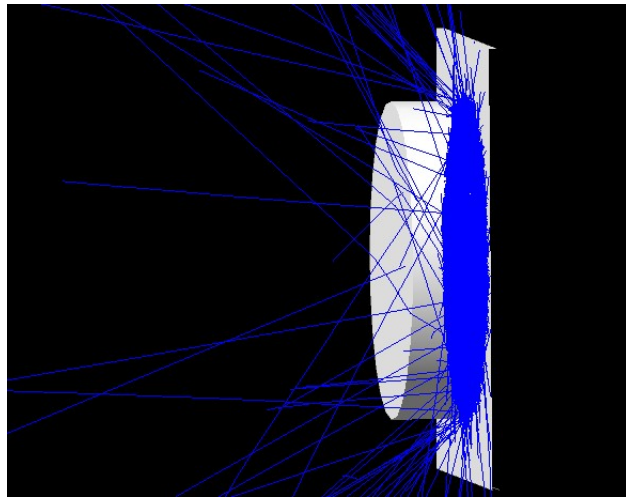


Figure 4: Geant4 simulation showing the trajectory of alpha particles emitted from a ^{225}Ac source. The alpha particles are distributed in $13\ \mu\text{m}$ water solution representing the cell diameter, passing through the Mylar foil. The blue lines represent the simulated paths of alpha particles, demonstrating their interactions and energy deposition within the detector setup.

3. Results and discussion

3.1. Alpha decay spectrum from ^{225}Ac calibration source

Figure 5 shows the alpha spectrum for ^{225}Ac obtained using the BAD detection system, revealing four distinct peaks for ^{225}Ac (5830 keV), ^{221}Fr (6340 keV), ^{217}At (7067 keV), and ^{213}Po (8376 keV). The detector has been calibrated using the highest energy flank of each peak, while the tail observed on the lower energy side is attributed to the energy loss of alpha particles as they pass through the Mylar foil and the air gap before reaching the detector. Calibration was performed with a ^{225}Ac source of known activity, dried directly onto the Mylar foil in the sample cup geometry, ensuring that energy shifts caused by the detector assembly (Mylar foil and air gap) are already accounted for. The overall detector efficiency across the entire energy range was calculated to be 37%.

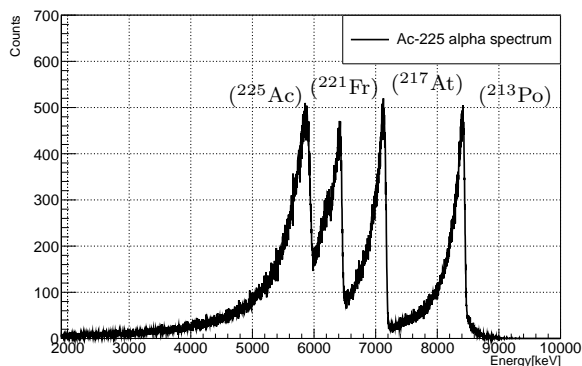


Figure 5: Alpha spectrum of ^{225}Ac obtained using the Bio-Sample Alpha Detector (BAD). The four distinct peaks correspond to the alpha decays of ^{225}Ac (5830 keV), ^{221}Fr (6340 keV), ^{217}At (7067 keV), and ^{213}Po (8376 keV). The spectrum demonstrates the clear detection of each isotope in the decay chain.

3.2. Cell Culture Distribution

Figure 6 shows the distribution of AR42J cells on the Mylar foil. The cells appear to be evenly distributed across the surface of the sample cup, with no visible clumping or aggregation. This even distribution is crucial for ensuring uniform exposure during alpha spectroscopy. Microspheres with a known diameter of $20.1\ \mu\text{m}$ were used as a reference, and the cell diameter was determined based on these microspheres using a microscope image and ImageJ software. A Gaussian fit was applied to the distribution, resulting in a cell diameter of $13.16 \pm 0.12\ \mu\text{m}$. Figure 7a shows the distribution of cell diameters in comparison with the microspheres.

The size of the cells is important because it ensures that alpha particles can exit the cells and reach the detector. An SRIM (Stopping and Range of Ions in Matter) simulation was performed to calculate the range of alpha particles in a water-based material, approximating the composition of the cells. Figure 7b shows the Bragg peak from the SRIM simulation, indicating that the range of alpha particles in water is approximately $50\ \mu\text{m}$. Given that the cell diameter is $13\ \mu\text{m}$, the simulation confirms that alpha particles can traverse the cells and exit into the detector. This is critical for measuring the uptake of alpha-emitting radiopharmaceuticals.

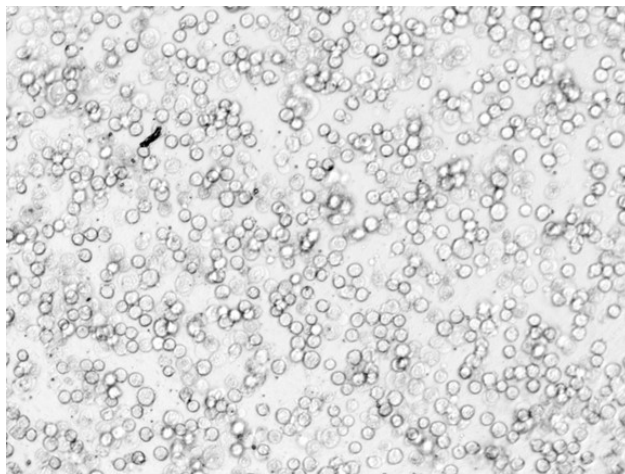


Figure 6: Microscopic image of AR42J rat pancreatic tumor cells in culture. The cells are shown adhering to the surface, displaying their characteristic round morphology. This image was taken before incubation with radiolabeled ^{225}Ac compounds for direct alpha spectroscopy.

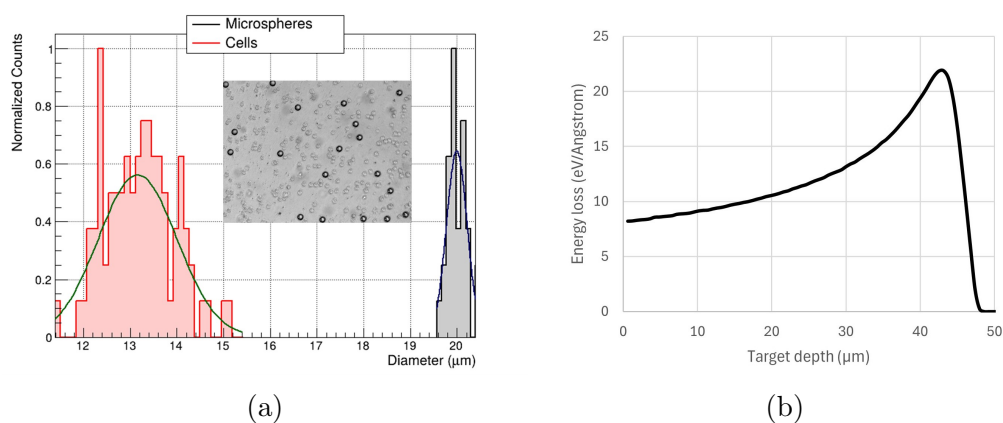


Figure 7: (a): Normalized distribution of microspheres and cells based on their diameter, with an inset showing a microscopic image of cells with reference spheres. Microspheres (black) have a diameter of 20 μm , while cells (red) show a wider distribution centered around $13.16 \pm 0.12 \mu\text{m}$. (b): Bragg peak showing the energy deposition of alpha particles in water, calculated using SRIM. The range of alpha particles in water is approximately 50 μm , confirming that alpha particles can exit AR42J cells (diameter $\sim 13 \mu\text{m}$) and be detected by the detector.

3.3. Alpha spectrum from cell sample incubated with ^{225}Ac Ac-crown-TATE

Figure 8a presents the alpha spectrum of ^{225}Ac Ac-crown-TATE from the cell sample, alongside the reference and cell supernatant samples, acquired using the BAD detection system. Figure 8b shows the logarithmic scale of the same spectrum. Although the detector

resolution does not clearly distinguish between the ^{225}Ac and ^{221}Fr peaks, the ^{217}At and ^{213}Po peaks are still recognizable. The number of counts was normalized to the initial activity measured by a calibrated HPGe detector, enabling a direct comparison between the three sample types. Three replicates of each sample were prepared, and the standard deviation is reflected in the plot. As can be seen in the cell sample spectrum, all peaks exhibit noticeable broadening, which is due to the energy loss of alpha particles as they traverse through the cells before reaching the detector. The spectrum shows significantly lower activity in the supernatant compared to the cell sample, indicating a clear uptake of activity by the cells. A small ^{213}Po peak is observed in the supernatant Figure 8b, which is likely due to the release of ^{213}Bi from the radiopharmaceutical complex into the media. This release might occur as a result of the high recoil energy generated during the alpha decay of ^{225}Ac , which can disrupt the coordination bonds within the radiopharmaceutical complex. Such disruption may lead to the dissociation of progeny isotopes, such as ^{213}Bi , from the original complex, allowing them to migrate into the surrounding media. The redistribution of daughter isotopes can affect both the therapeutic efficacy and dosimetry, as the progenies may accumulate in off-target tissues or regions. When comparing the ^{213}Po peak in the cell sample and the supernatant, a shift to lower energies is observed in the cell sample spectrum. This shift is attributed to the presence of cells in the sample, which cause additional energy loss for alpha particles, whereas such interactions are absent in the supernatant. The reference sample, which contains no cells, exhibits very low activity, suggesting that the washing procedure effectively removed free activity that was not taken up by the cells.

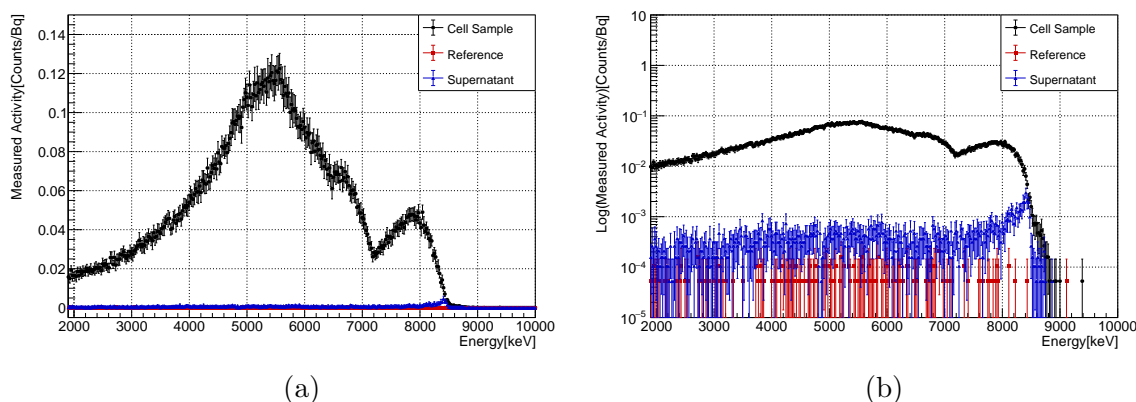


Figure 8: Alpha spectra of $[^{225}\text{Ac}]\text{Ac-crown-TATE}$ obtained from the cell sample (black), supernatant (blue), and reference sample (red, no cells), and (a): Linear scale. (b): Logarithmic scale.

3.4. Alpha spectrum from cell sample incubated with $[^{225}\text{Ac}]\text{Ac}^{3+}$

The uptake of free $[^{225}\text{Ac}]\text{Ac}^{3+}$ in AR42J cells was studied and the alpha spectra of cells alongside supernatant and the reference (no cells) were acquired using the BAD detection

system as shown in Figure 9a. These plots indicate that there is uptake of free $[^{225}\text{Ac}]\text{Ac}^{3+}$ in the cells but less than $[^{225}\text{Ac}]\text{Ac-crown-TATE}$. By comparing the spectra of the cell sample and the supernatant, it is evident that free $[^{225}\text{Ac}]\text{Ac}^{3+}$ is present in the supernatant, suggesting partial uptake of the isotope by the cells. As expected, the reference sample, which contains no cells, shows minimal activity, confirming that the washing procedure effectively removes unbound activity.

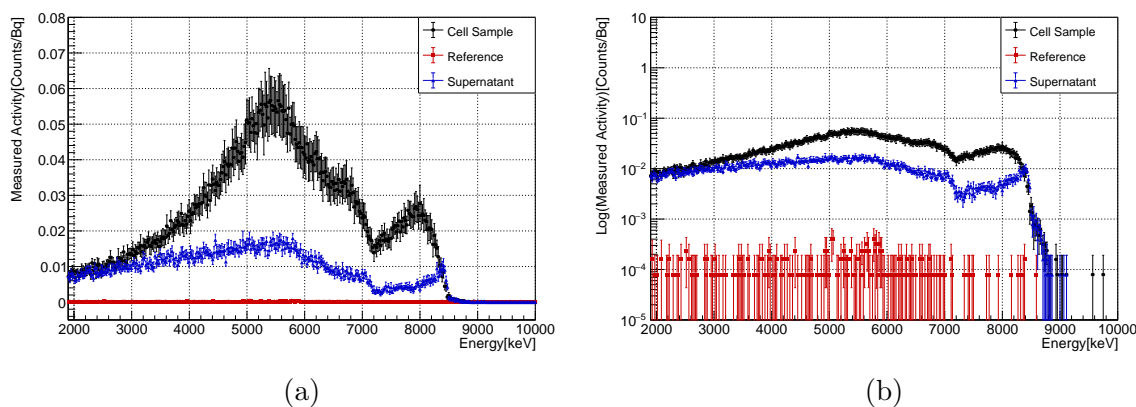


Figure 9: Alpha spectra of free $[^{225}\text{Ac}]\text{Ac}^{3+}$ obtained from the cell sample (black), supernatant (blue), and reference sample (red, no cells), and (a): Linear scale. (b): Logarithmic scale.

3.5. Alpha spectrum from cell sample incubated with $[^{225}\text{Ac}]\text{Ac-PSMA-617}$

As a negative control, the behavior of $[^{225}\text{Ac}]\text{Ac-PSMA-617}$ on AR42J cell cultures was investigated. Figure 10 shows the alpha spectrum of $[^{225}\text{Ac}]\text{Ac-PSMA-617}$ from the cell sample, along with the reference and cell supernatant samples, acquired using the BAD detection system in linear scale, while Figure 10b presents the spectrum on a logarithmic scale. Since AR42J cells lack receptors for the PSMA-617 ligand, minimal uptake of $[^{225}\text{Ac}]\text{Ac-PSMA-617}$ by the cells was expected. The alpha spectrum from the cell sample is almost identical to that of the supernatant, suggesting that $[^{225}\text{Ac}]\text{Ac-PSMA-617}$ remained largely unbound and free in the medium, with minimal cellular uptake. The reference sample, which lacks cells, shows very low activity, confirming that the washing procedure effectively removed unbound $[^{225}\text{Ac}]\text{Ac-PSMA-617}$, emphasizing the absence of significant binding to AR42J cells. The different shape of the ^{213}Po peak in the supernatant and cell sample is related to the presence of cells, which causes an energy shift and broadening of the spectrum.

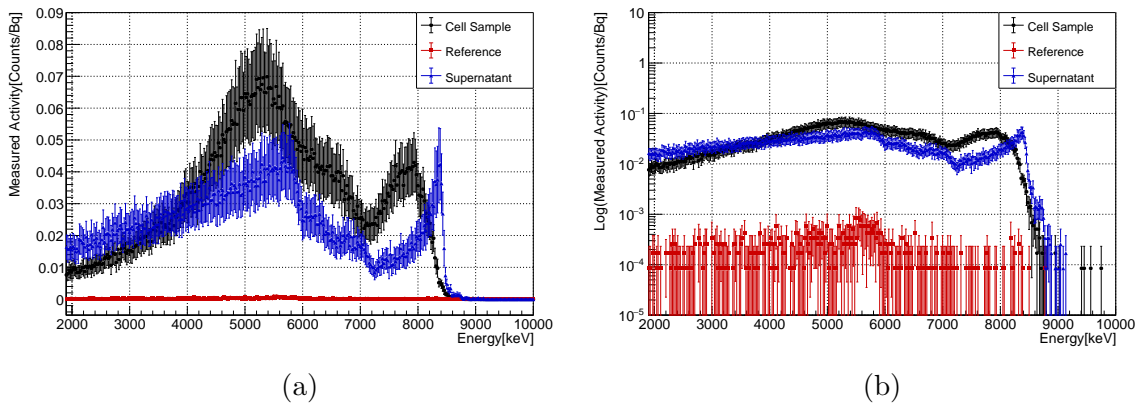


Figure 10: Alpha spectra of $[^{225}\text{Ac}]\text{Ac-PSMA-617}$ obtained from the cell sample (black), reference sample (red), and supernatant (blue). (a): Linear scale. (b): Logarithmic scale.

3.6. Geant4 simulation

Figure 11 shows a comparison between the experimental and simulated spectra for ^{225}Ac distributed on Mylar foil near the detector. The four characteristic peaks of the ^{225}Ac decay chain ^{225}Ac (5830 keV), ^{221}Fr (6340 keV), ^{217}At (7067 keV), and ^{213}Po (8376 keV) are clearly distinguishable. The simulation and experimental data are well-aligned, with a particularly strong match at the ^{213}Po peak. The slight discrepancies observed in the other peaks may be attributed to minor differences in the physical setup, such as detector response or material variations in the sample cup that were not fully captured in the simulation.

Figure 12 compares the experimental and simulated spectra for ^{225}Ac distributed in the cell medium. In the Geant4 simulation, ^{225}Ac was modeled as being randomly distributed in an aqueous solution with a thickness of 13 μm , representing the approximate diameter of the cells. The experimental and simulated spectra show good agreement, confirming the behavior of ^{225}Ac in solution. This alignment demonstrates that the simulation accurately models the energy deposition and supports the validity of the experimental approach. It is important to highlight that a 300 keV shift was applied to the simulation data to account for energy loss caused by the Mylar foil, as calculated using the SRIM software. This energy loss is not observed in the experimental data because the detector was calibrated with the Mylar foil in place. This calibration inherently compensates for the energy loss, ensuring accurate energy measurements in the experimental spectrum.

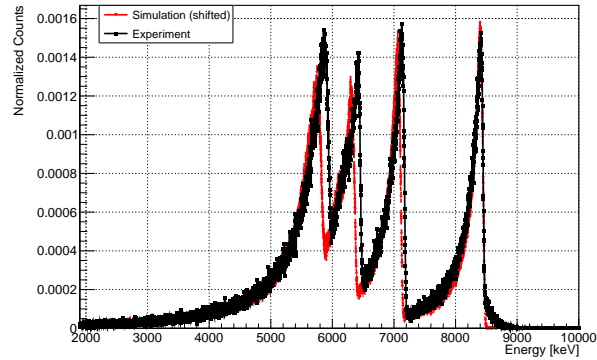


Figure 11: Comparison of experimental and simulated alpha spectra for dried ^{225}Ac placed on Mylar foil near the detector.

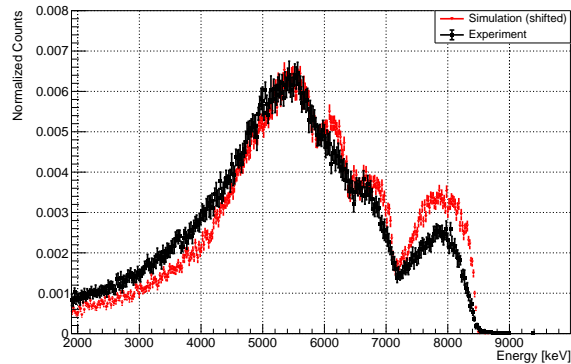


Figure 12: Comparison of experimental and simulated alpha spectra for ^{225}Ac randomly distributed in an aqueous solution, representing cell samples with a thickness of 13 μm .

4. Conclusion and Outlook

To the best of our knowledge, this study is the first to use an alpha detector for direct alpha spectroscopy of cancer cell samples under ambient conditions, demonstrating the potential of the Bio-Sample Alpha Detector (BAD) as a novel method in this context. The method enabled direct measurement of alpha spectra from AR42J rat pancreatic tumor cells incubated with $[^{225}\text{Ac}]\text{Ac-crown-TATE}$ and $[^{225}\text{Ac}]\text{Ac-PSMA-617}$ and $[^{225}\text{Ac}]\text{Ac}^{3+}$. Results indicate significant uptake of $[^{225}\text{Ac}]\text{Ac-crown-TATE}$ by the cells, evidenced by distinct alpha spectra and minimal activity in the supernatant, suggesting efficient retention. In contrast, less efficient uptake of $^{225}\text{Ac-PSMA-617}$ was observed, correlating with the lack of PSMA-617 receptors on AR42J cells.

Detection of ^{213}Po , a decay product of ^{225}Ac , serves as an indicator of ^{213}Bi redistribution from the cells into the surrounding media. This redistribution impacts dosimetry and

toxicity, as progeny isotopes like ^{213}Bi can migrate to off-target tissues, potentially increasing toxicity risks. The well-documented kidney toxicity of ^{213}Bi [21] underscores the importance of understanding and mitigating this redistribution to optimize the therapeutic index of radiopharmaceuticals. Geant4 simulations validated experimental results and provided insights into alpha particle interactions with biological samples.

This work underscores BAD’s versatility in conducting sensitive, real-time measurements of radiopharmaceuticals in cancer cells, enhancing understanding of radionuclide behavior in biological environments.

Future studies can explore additional cell types, radiolabeled compounds, and improved detector designs. Integration of a CO_2 incubator and multi-channel data acquisition system will facilitate simultaneous measurements for statistically relevant systematic studies. A peristaltic pump system to control radiolabeled compound flow through cell cultures will simulate vascular conditions, providing insights into *in vivo* behavior of Targeted Alpha Therapy (TAT) agents. This study serves as an introduction to the BAD detector and method as an option for direct alpha spectroscopy. However, further optimization of the detector’s behavior for actual cell studies is essential to fully harness its potential for advancing TAT research and clinical applications.

Acknowledgements

TRIUMF receives federal funding via a contribution agreement through the National Research Council of Canada. We also acknowledge added support through the New Frontiers in Research Fund - Exploration NFRFE-2019-00128 and Discovery Grants from the Natural Sciences and Engineering Research Council of Canada, (NSERC): SAPIN-2021-00030 (P. Kunz) and RGPIN-2022-03887 (H. Yang). Many thanks to the Life Science Laboratory team.

References

- [1] V. Radchenko, A. Morgenstern, A. R. Jalilian, C. F. Ramogida, C. Cutler, C. Duchemin, C. Hoehr, F. Haddad, F. Bruchertseifer, H. Gausemel, et al., Production and supply of α -particle-emitting radionuclides for targeted α -therapy, *Journal of nuclear medicine* 62 (11) (2021) 1495–1503.
- [2] A. Jang, A. T. Kendi, G. B. Johnson, T. R. Halfdanarson, O. Sartor, Targeted alpha-particle therapy: a review of current trials, *International journal of molecular sciences* 24 (14) (2023) 11626.
- [3] R. Eychenne, M. Chérel, F. Haddad, F. Guérard, J.-F. Gestin, Overview of the most promising radionuclides for targeted alpha therapy: The “hopeful eight”, *Pharmaceutics* 13 (6) (2021) 906.
- [4] B. J. Allen, C.-Y. Huang, R. A. Clarke, Targeted alpha anticancer therapies: update and future prospects, *Biologics: Targets and Therapy* (2014) 255–267.
- [5] M. Sollini, K. Marzo, A. Chiti, M. Kirienko, The five “w” s and “how” of targeted alpha therapy: why? who? what? where? when? and how?, *Rendiconti Lincei. Scienze Fisiche e Naturali* 31 (2020) 231–247.
- [6] M. Miederer, D. A. Scheinberg, M. R. McDevitt, Realizing the potential of the actinium-225 radionuclide generator in targeted alpha particle therapy applications, *Advanced drug delivery reviews* 60 (12) (2008) 1371–1382.

- [7] J. Kleynhans, T. Ebenhan, F. Cleeren, M. M. Sathekge, Can current preclinical strategies for radiopharmaceutical development meet the needs of targeted alpha therapy?, *European Journal of Nuclear Medicine and Molecular Imaging* (2024) 1–16.
- [8] E. L. Hooijman, V. Radchenko, S. W. Ling, M. Konijnenberg, T. Brabander, S. L. Koolen, E. de Blois, Implementing ac-225 labelled radiopharmaceuticals: practical considerations and (pre-) clinical perspectives, *EJNMMI Radiopharmacy and Chemistry* 9 (1) (2024) 9.
- [9] L. Wharton, S. W. McNeil, H. Merkens, Z. Yuan, M. Van de Voorde, G. Engudar, A. Ingham, H. Koniar, C. Rodríguez-Rodríguez, V. Radchenko, et al., Preclinical evaluation of [155/161tb] tb-crown-tate—a novel spect imaging theranostic agent targeting neuroendocrine tumours, *Molecules* 28 (7) (2023) 3155.
- [10] A. K. Robertson, B. L. McNeil, H. Yang, D. Gendron, R. Perron, V. Radchenko, S. Zeisler, P. Causey, P. Schaffer, 232th-spallation-produced 225ac with reduced 227ac content, *Inorganic Chemistry* 59 (17) (2020) 12156–12165.
- [11] H. Yang, C. Zhang, Z. Yuan, C. Rodriguez-Rodriguez, A. Robertson, V. Radchenko, R. Perron, D. Gendron, P. Causey, F. Gao, et al., Synthesis and evaluation of a macrocyclic actinium-225 chelator, quality control and in vivo evaluation of 225ac-crown- α msh peptide, *Chemistry—A European Journal* 26 (50) (2020) 11435–11440.
- [12] H. Photonics, S3204-09 si photodiode, <https://www.hamamatsu.com/us/en/product/optical-sensors/photodiodes/si-photodiodes/S3204-09.html>, accessed: Oct. 01, 2024.
- [13] P. Kunz, C. Andreoiu, P. Bricault, M. Dombisky, J. Lassen, A. Teigelhöfer, H. Heggen, F. Wong, Nuclear and in-source laser spectroscopy with the isac yield station, *Review of Scientific Instruments* 85 (5) (2014).
- [14] P. Kunz, C. Andreoiu, V. Brown, M. Cervantes, J. Even, F. H. Garcia, A. Gottberg, J. Lassen, V. Radchenko, C. F. Ramogida, et al., Medical isotope collection from isac targets, in: *EPJ Web of Conferences*, Vol. 229, EDP Sciences, 2020, p. 06003.
- [15] C. F. Ramogida, A. K. Robertson, U. Jermilova, C. Zhang, H. Yang, P. Kunz, J. Lassen, I. Bratanovic, V. Brown, L. Southcott, et al., Evaluation of polydentate picolinic acid chelating ligands and an α -melanocyte-stimulating hormone derivative for targeted alpha therapy using isol-produced 225 ac, *EJNMMI Radiopharmacy and Chemistry* 4 (2019) 1–20.
- [16] A. K. Robertson, A. Lobbezoo, L. Moskven, P. Schaffer, C. Hoehr, Design of a thorium metal target for 225ac production at triumph, *Instruments* 3 (1) (2019) 18.
- [17] A. Ingham, L. Wharton, H. Koniar, H. Merkens, S. McNeil, S. Sekar, M. Osooly, C. Rodríguez-Rodríguez, F. Bénard, P. Schaffer, et al., Preclinical evaluation of [225ac] ac-crown-tate—an alpha-emitting radiopharmaceutical for neuroendocrine tumors, *Nuclear Medicine and Biology* 138 (2024) 108944.
- [18] P. Thakral, J. Simecek, S. Marx, J. Kumari, V. Pant, I. B. Sen, In-house preparation and quality control of ac-225 prostate-specific membrane antigen-617 for the targeted alpha therapy of castration-resistant prostate carcinoma, *Indian Journal of Nuclear Medicine* 36 (2) (2021) 114–119.
- [19] ATCC, AR42J (ATCC® CRL-1492™), Accessed: Oct. 01, 2024. [Online]. Available: <https://www.atcc.org/products/crl-1492> (2024).
- [20] S. Agostinelli, J. Allison, K. a. Amako, J. Apostolakis, H. Araujo, P. Arce, M. Asai, D. Axen, S. Banerjee, G. Barrand, et al., Geant4—a simulation toolkit, *Nuclear instruments and methods in physics research section A: Accelerators, Spectrometers, Detectors and Associated Equipment* 506 (3) (2003) 250–303.
- [21] J. Schwartz, J. Jaggi, J. O’donoghue, S. Ruan, M. McDevitt, S. Larson, D. Scheinberg, J. Humm, Renal uptake of bismuth-213 and its contribution to kidney radiation dose following administration of actinium-225-labeled antibody, *Physics in Medicine & Biology* 56 (3) (2011) 721.